Effect of Line Width Roughness on Optical Scatterometry Measurements

Brent C. Bergner,[1,2,3] Thomas A. Germer,[1] and Thomas J. Suleski[2]

[1]*National Institute of Standards and Technology, Gaithersburg, MD 20899*
[2]*Department of Physics and Optical Science, University of North Carolina, Charlotte, NC 28223*
[3]*KT Consulting, Inc., Antioch, CA 94509*

ABSTRACT

Line width roughness (LWR) has been identified as a potential source of uncertainty in scatterometry measurements, and characterizing its effect is required to improve the method's accuracy and to make measurements traceable. In this work, we extend previous work by using rigorous coupled wave (RCW) analysis on two-dimensionally periodic structures to examine the effects of LWR. We compare the results with simpler models relying upon a number of effective medium approximations. We find that the effective medium approximations yield an approximate order of magnitude indicator of the effect, but that the quantitative agreement may not be good enough to include in scatterometry models.

Keywords: effective medium approximation, line width roughness, scatterometry

1. INTRODUCTION

Optical scatterometry is becoming an increasingly important tool for dimensional semiconductor metrology. Line width roughness (LWR) has been identified as a potentially significant source of uncertainty, and characterizing its effect on scatterometry measurements is required to improve the accuracy and to make the method traceable [1, 2].

Previous work on line edge roughness and line width roughness has examined scattering from gratings with long wavelength roughness, where the characteristic correlation length of the roughness is greater than the period of the grating and the wavelength of the light. Boher and Petit [3] used optical Fourier transform scatterometry to examine the scattering from structures that exhibited edge roughness. Since this technique compares signals from multiple diffraction orders, it is only useful for measuring roughness with periods that are greater than the probe wavelength. Germer [4] simulated line variations by applying rigorous coupled-wave (RCW) analysis to one-dimensionally periodic structures containing multiple random lines and compared the average of these results to an approximation, whereby the signature was calculated by averaging the reflected field over a distribution of linewidths. He achieved reasonable agreement for long period roughness.

The effect of short period LWR on optical scatterometry signals could be simulated using a rigorous coupled wave analysis for a two-dimensionally periodic structure (2D RCW). However, the computational expense needed to model edge roughness in this way can be prohibitive. For example, if one retains ±10 orders in each of the two dimensions of the field expansions, the calculation is about 9000 times slower than if one retained ±10 orders in just the grating direction using RCW for one-dimensionally periodic structures (1D RCW). An approximation that enables an estimate of the effects of LWR, without requiring a full 2D RCW simulation, would allow such effects to be accounted for in scatterometry measurements.

In this paper, we use a 2D RCW analysis to examine the effects of LWR having characteristic correlation lengths that are less than the grating period and compare the results to those obtained using various effective medium theories.

2. APPROACH

In this paper, we calculate the reflection of a rough periodic grating with full three-dimensional solutions to Maxwell's equations and compare the results to effective medium approximations that only require a two-dimensional solution. The two-dimensional solutions rely upon RCW analysis of one-dimensionally periodic gratings [5-8]. The

software for the RCW analysis is available online [9]. The three-dimensional solutions rely upon RCW analysis of two-dimensionally periodic gratings [10].

We studied a nominal grating consisting of simple lines with vertical sidewalls shown in Fig. 1(a). We varied the nominal line material, width w, height h, and the period P_x of the grating, but always assumed a silicon substrate. To simulate roughness, we considered the structure shown in Fig. 1(b), where we added a square wave modulation to the sidewall position. The sides of the line were modulated in opposite directions, corresponding to what is often referred to as line-width roughness (LWR). We kept the mean line width constant, and the duty cycle of the modulation fixed at 50 %. The period of the modulation, P_y, and the peak-to-peak amplitude, a, were also varied. We define $q = 2a/P_y$ as the aspect ratio of the roughness. We performed the three-dimensional calculations on these structures.

To model the roughness, we considered the structure shown in Fig. 1(c), where we approximate the modulated regions as effective medium layers. The structure shown in Fig. 1(c) can be solved with a two-dimensional solution to Maxwell's equations, at a significant computational cost savings.

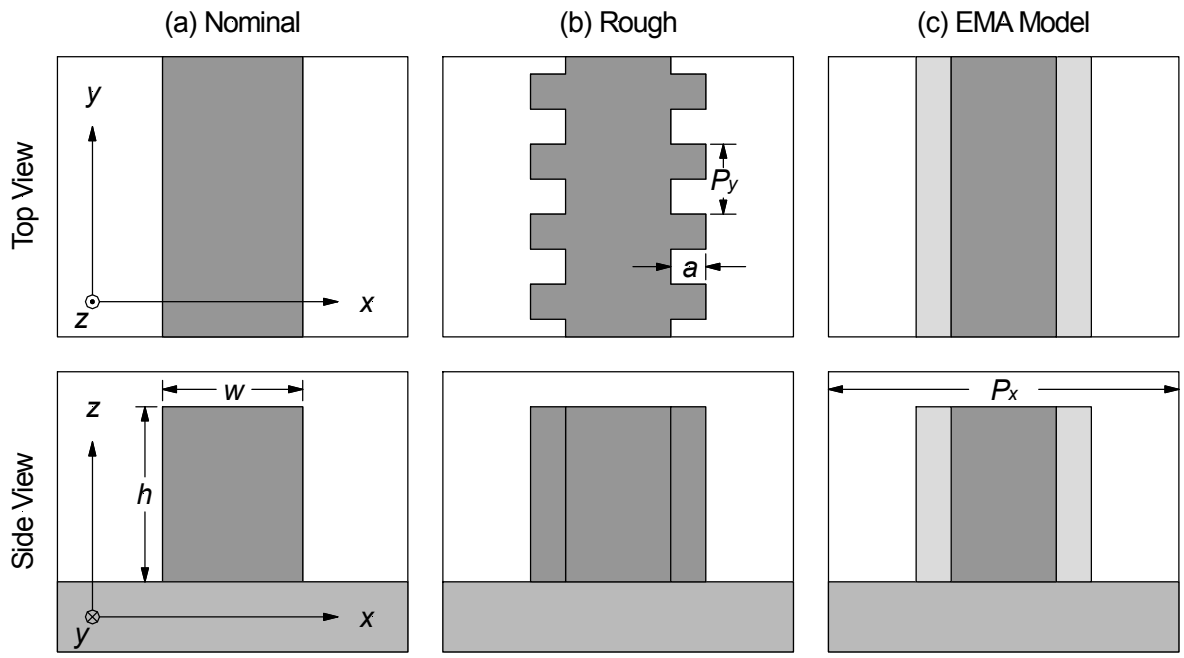

Figure 1. Examples the index profiles within a one period by one period cell used in the simulations. The figures show (a) the nominal profile, (b) a 2D periodic profile used to directly calculate the effect of LWR using a 2D RCW simulation, and (c) a 1D periodic profile used to approximate the effect of the LWR with an effective medium layer. Profiles with a large peak to valley roughness are shown for clarity. Much smaller roughness amplitudes were used in the simulations. The dark areas correspond to areas containing the grating material, the gray area corresponds to the effective medium layer, and the light areas correspond to areas containing the fill material.

In RCW analysis, the electric and magnetic fields are each expanded in a Floquet series. RCW models converge on an exact solution when the number of Floquet expansion orders (G) that are retained for the calculation approaches infinity. However, the number of operations that are needed for the computation is proportional to G^3. In order to make the computation tractable, the number of orders must be limited. While we can perform more accurate simulations for the simpler, one-dimensionally periodic gratings, we chose to use the same number of orders in each dimension for both the one-dimensionally and the two-dimensionally periodic gratings. We chose to truncate the expansion to ±10 orders in each dimension, corresponding to a total of 21 orders for the one-dimensionally periodic gratings and 441 orders for the two-dimensionally periodic gratings.

The optical properties of composite materials can be approximated by a uniform effective medium when the length scales associated with the local variations in permittivity are small compared to the wavelength in the media. The reflection and transmission coefficients of a rough surface are often calculated by replacing the rough interface by a thin

film having a thickness related to the amplitude of the roughness and a permittivity derived from an appropriate effective medium approximation (EMA). In a similar manner, we hope to be able to use an EMA to approximate the effects of line width roughness. In this section, we describe two families of EMAs, which we considered for this application.

The first EMA type starts with a relationship, derived from the Clausius-Mossotti equation that has been generalized using the expression for the polarizability for ellipsoidal inclusions [11],

$$\frac{\varepsilon_{\text{eff}} - \varepsilon_0}{\varepsilon_{\text{eff}} + L(\varepsilon_0 - \varepsilon_{\text{eff}})} = \sum_{i=1}^{N} f_i \frac{\varepsilon_i - \varepsilon_0}{\varepsilon_i + L(\varepsilon_0 - \varepsilon_i)} \tag{1}$$

where ε_{eff} is the effective medium permittivity, ε_0 is the permittivity of the host medium, and ε_i and f_i are the permittivities and volume fractions of each of the N inclusion materials. The geometrical factor L depends upon the shape of the ellipsoidal inclusions and the direction of the electric field: for spheres, $L_x = L_y = L_z = 1/3$, for highly prolate ellipsoids (needles) aligned along the z direction, $L_x = L_y = 1/2$ and $L_z = 0$, and for highly oblate ellipsoids (plates) aligned along the y direction $L_x = L_z = 0$ and $L_y = 1$. The Bruggeman model puts all of the constituent materials on an equal footing. The host permittivity ε_0 is the same as the effective medium permittivity ε_{eff}, and the volume fractions of the constituent materials sum to one. Thus, for $N = 2$, we can solve Eq. (1) for the effective permittivity,

$$\varepsilon_{\text{eff}} = \frac{\varepsilon_1(f_1 - L) + \varepsilon_2(f_2 - L) \pm \sqrt{\left[\varepsilon_1(f_1 - L) + \varepsilon_2(f_2 - L)\right]^2 - 4\varepsilon_1\varepsilon_2 L(L-1)}}{2(1-L)} \tag{2}$$

The sign is chosen to ensure a sensible result. For $L = 0$, the result simplifies to

$$\varepsilon_{\text{eff}} = \varepsilon_1 f_1 + \varepsilon_2 f_2 \tag{3}$$

while for $L = 1$, the result simplifies to

$$\varepsilon_{\text{eff}} = \frac{\varepsilon_1 \varepsilon_2}{\varepsilon_1 f_1 + \varepsilon_2 f_2} \tag{4}$$

The result for spheres ($L = 1/3$ for all directions) is the common isotropic Bruggeman EMA (IBEMA). The isotropic Bruggeman effective medium approximation is used extensively to model interfacial roughness in ellipsometry measurements of thin film stacks [12-14]. However, an anisotropic model might be better for modeling edge roughness since this type of roughness tends to have a preferred orientation with respect to the grating vector. The Bruggeman effective medium approximation can be made anisotropic by allowing different geometrical factors for two or more directions in Eq. (2). One reasonable approach for LWR is to consider an effective medium layer made up of needles aligned along the z-direction ($L_x = L_y = 1/2$ and $L_z = 0$). We will refer to this model as the anisotropic Bruggeman EMA (ABEMA).

Another approach is to consider the roughness to be made up of plates aligned in the y direction ($L_x = 0$, $L_y = 1$ and $L_z = 0$). We will refer to this second model as the form birefringence EMA (FBEMA), because it is equivalent to the form birefringence model for a sub-wavelength lamellar grating derived in Born and Wolf [15] by considering the continuity of the electric field within a regular assembly of parallel plates. In this case, we assume that the composite material is stratified, with layers having thickness very small compared to the wavelength and alternating between the two materials. To match the boundary conditions at the interfaces, we require that the volume-mean electric field be constant when the electric field is parallel to the layers and that the volume-mean electric displacement be constant when the electric field is perpendicular to the layers. Using these arguments, we find that the effective permittivities yield the same results as the Bruggeman EMA for plates with normals aligned along the y direction, given by Eqs. (3) and (4) above, respectively. These results are also equivalent to the results obtained by Yariv and Yeh [16] by neglecting higher order terms in a series expansion in their expression for the dispersion relationship of Bloch waves in periodic media, to the results obtained by Southwell [17] in analogy to the dispersion relationship for periodic thin films, and to the results obtained by Rytov [18] in considering an approximation for multiple scattering in a stratified media.

Figure 2 shows the effective optical constants n and k as functions of composition for the different EMAs for mixtures of vacuum and silicon. We see that we can obtain a wide range of effective indices and that there is significant birefringence in all but the IBEMA case.

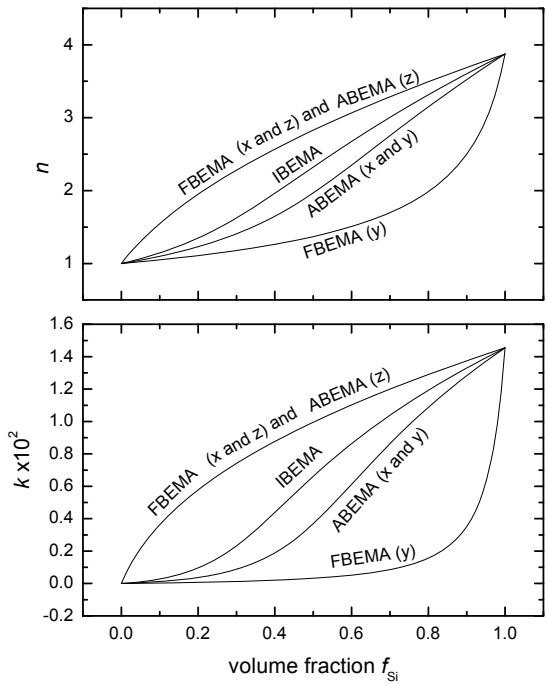

Figure 2. Optical constants, n and k, for the effective medium approximations described in the text. The components are assumed to be silicon and vacuum, evaluated at 633 nm

Form birefringence has been suggested in the past for modeling line edge roughness [19]. However, two important assumptions were made in deriving the expressions for form birefringence, Eqs. (3) and (4): (a) the period of the grating is small compared with the wavelength of the incident light, and (b) the amplitude of the roughness is large compared to its period. These conditions imply high aspect ratio roughness, i.e. $q >> 1$, a condition that would not be expected to occur often for LWR.

3. RESULTS

Figure 3 shows the predicted angle-resolved reflectance for a grating, consisting of 100 nm wide, 200 nm high silicon lines with a pitch of 200 nm on a silicon substrate, in air, probed with a wavelength of 633 nm. The sidewalls of the lines are vertical. The grating is oriented such that the grating vector lies in the plane of incidence (classical mounting). The electric field for s-polarization (often called transverse-electric or TE polarization) and the magnetic field for p-polarization (often called transverse-magnetic or TM polarization) are normal to the grating vector and parallel to the lines.

When we apply small amounts of roughness to this grating, we will be perturbing these reflectance curves by a small amount. Thus, the effects of line width roughness on the signal are best observed by showing the differences between signals calculated for rough gratings and those calculated from the nominal, unperturbed grating. Figure 4 shows these reflectance differences calculated using the 2D RCW theory applied to LWR with a period of P_y = 10 nm and amplitudes a between 1 nm and 5 nm. The reflectance differences are larger for some incident angles than for others, but generally

increase, as expected, with roughness amplitude. For this particular grating, the p-polarized reflectance is much less sensitive to the roughness than the s-polarized reflectance. Graphs of the reflectance differences calculated using the various effective medium models show similar behavior.

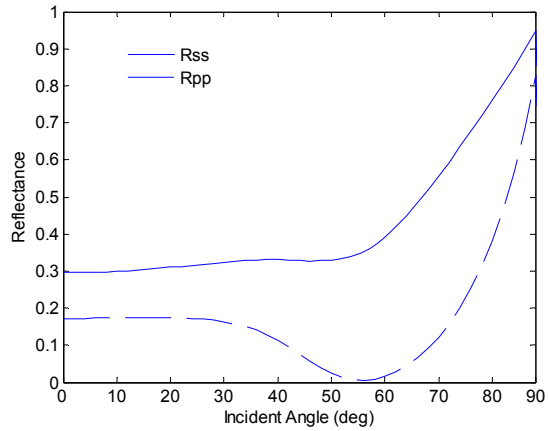

Figure 3. Reflectance for the nominal grating described in the text as a function of incident angle for (solid line) s-polarization and (dashed line) p-polarization.

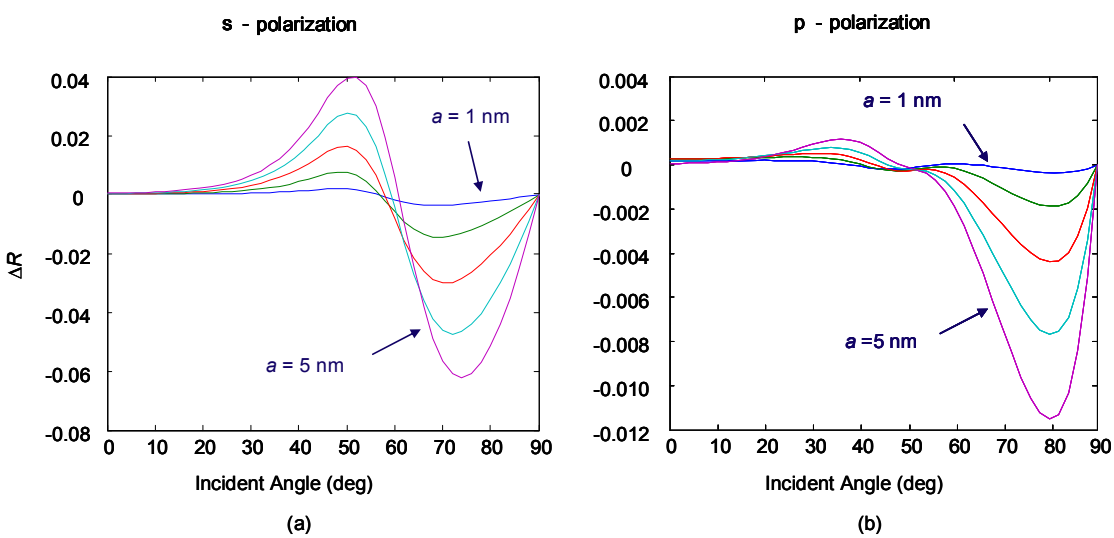

Figure 4. Difference between reflectance calculated for the nominal grating (with no roughness) and gratings with various roughness amplitudes a from 0 nm to 5 nm. The curves are calculated for gratings with a 10 nm period roughness for (a) s-polarization and (b) p-polarization. Note the difference in scales.

We can visually assess the effectiveness of an EMA model by graphing reflectance differences, ΔR, calculated using the EMA model against those calculated using the 2D RCW model. Figure 5 shows this comparison for each polarization and for the IBEMA, the FBEMA, and the ABEMA for roughness amplitude a = 10 nm and roughness period P_y = 10 nm. If an approximate EMA model were valid, then the relationship between the EMA model and the 2D RCW model should be a straight line with unit slope. It is clear from figure 5 that none of the EMA models match the 2D RCW calculations perfectly, but that some are better than others. For example, the isotropic Bruggeman model is particularly poor. For this grating, the anisotropic Bruggeman model seems to visually agree best with the 2D RCW calculations.

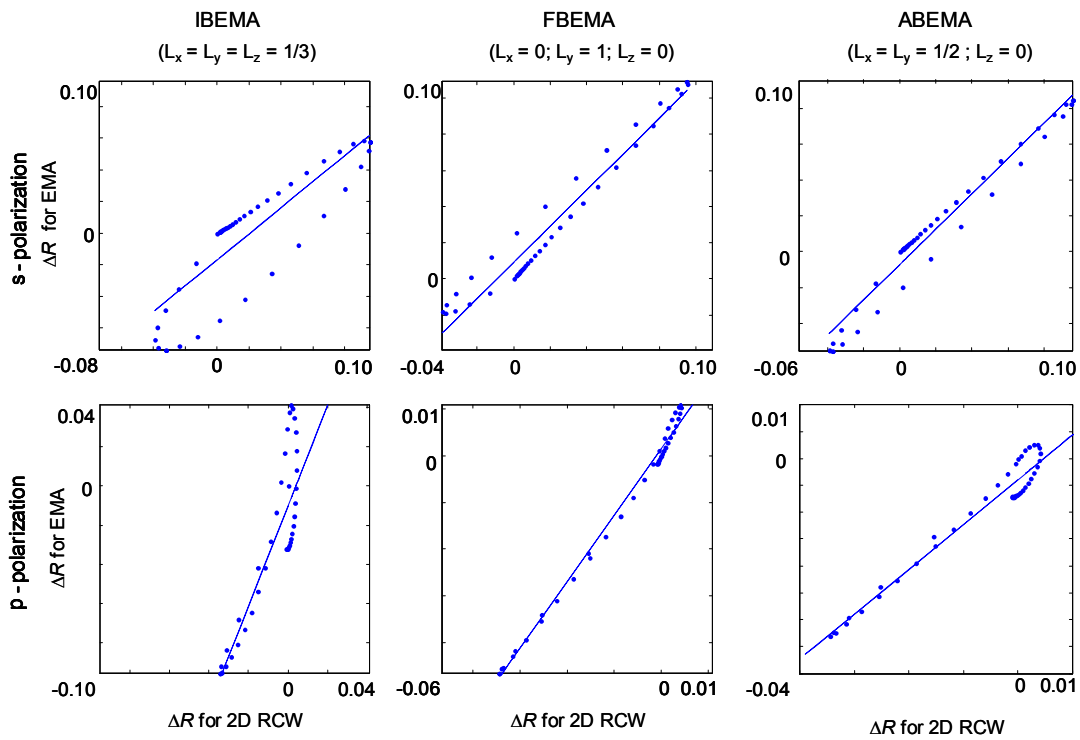

Figure 5. The reflectance difference calculated for the three effective medium approximations as a function of that calculated using the 2D RCW model. Each data point corresponds to a different angle of incidence. For clarity, only results for a = 10 nm and P_y = 10 nm are shown. The best fit line is included with each graph

The slope of the best fit line, b, and the linear correlation coefficient, r, of these plots [20] can be used to quantify the degree of suitability of each model. A linear correlation coefficient of one indicates a good fit. A slope of one indicates that there is a one to one correspondence between the roughness amplitude and the thickness of the effective medium layer that best approximates the roughness. The model could still be useful if the slope is not one, but the slope should be constant over the relevant range of roughness amplitudes and periods. Figure 6 shows a comparison of the linear correlation coefficient for the FBEMA and ABEMA as a function of the roughness period and aspect ratio.

Figure 6(a) indicates that the correlation coefficient reaches stable values for roughness periods below approximately 60 nm (approximately one-tenth of the incident wavelength) for both the FBEMA and the ABEMA. The slopes of the lines also approach unity, but more slowly for the FBEMA for the s-polarization, in this case. Figures 6(a) and 6(b) are plotted for a = 10 nm. The reason for displaying the results for such a large roughness values can be seen by examining Figs. 6(c) and 6(d); the models begin to break down when the roughness amplitude reaches approximately half of the roughness period.

4. DISCUSSION

The isotropic Brugemman EMA was generally very poor, but the form birefringence and the anisotropic Bruggeman EMAs were each effective to various degrees for different grating cases that we studied. However, we were unable to find a single EMA that could effectively model LWR for both polarizations over a wide range of roughness periods and amplitudes and grating geometries. In the future, we hope to develop heuristics that can be used to decide which model would be most appropriate for a specific grating, the roughness type, and the roughness amplitude.

The ABEMA and FBEMA models begin to break down for small aspect ratios (q less than about 0.5). This observation is consistent with the assumption made in the derivation of the FBEMA that the lateral extent of the plates (amplitude of the roughness) is large compared with the distance between the plates. This condition would require roughness slopes large compared to the mean line edge, a condition not expected to occur in microlithography. In such

cases, a perturbation method might be more appropriate, but not as simple to implement or as computationally efficient as an EMA.

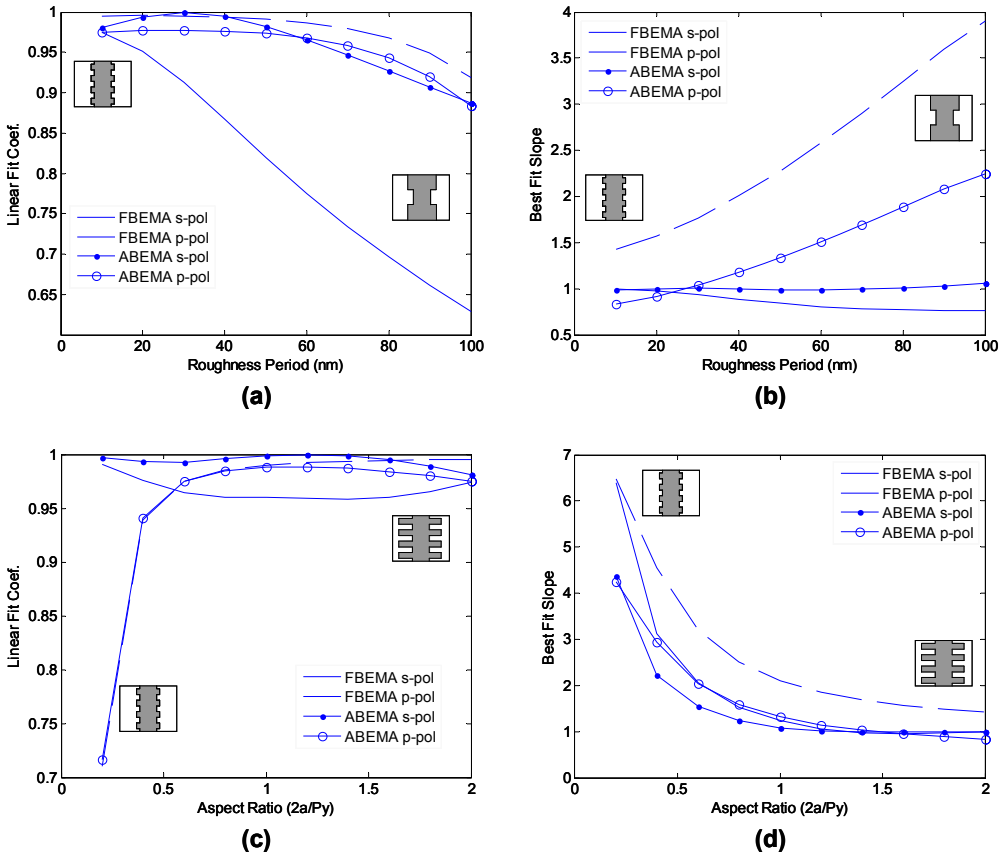

Figure 6. Linear correlation coefficients (in a and c) and best fit slopes (in b and d) for linear fits of reflectance differences calculated using an EMA model versus those using 2D RCW. Graphs (a) and (b) show the relationships with respect to roughness period for a = 10 nm. Graphs (c) and (d) show the relationships as a function of aspect ratio q for a roughness period P_y = 10 nm. The curves correspond to (solid lines) FBEMA, s-polarization, (dashed lines) FBEMA, p-polarization, (solid dots) ABEMA, s-polarization, and (circles) ABEMA, p-polarization. Inset cartoons are meant to loosely represent the relative dimensions of the roughness profile.

For simplicity, we chose to limit this discussion to square-wave modulations of the line edge. Results for LWR with a sinusoidal profile show a similar dependence on the roughness period and aspect ratio for both the FBEMA and ABEMA. Notably missing from this work are the effects of random roughness. Random roughness is much more likely to occur naturally and may behave differently than square-wave roughness. The effects of random roughness are not expected to be dramatically different, but are more difficult to model, because of the longer periods P_y required, the need to average over realizations of the random line edge function, and the different power spectral density functions that need to be considered.

5. CONCLUSIONS

The ability to use an effective medium approximation to model LWR using a RCW algorithm for one-dimensionally periodic structure can significantly reduce the computation time needed to model LWR. A comparison of the change of the reflectance function of a rigorous model of a grating with roughness to the change predicted by a model using an effective medium approximation for the LWR indicates that both the FBEMA and ABEMA are good candidates for modeling LWR when the period of the roughness is small (less than one-tenth of the incident wavelength) and the aspect ratio of the roughness is larger than 2. These constraints limit the usefulness of these EMAs for modeling LWR for optical scatterometry measurements. However, while the correlations are not perfect, they do provide rough order of magnitude estimates of the effects of LWR on optical scatterometry signals that can be used to estimate the errors in optical scatterometry measurements that might result from LWR.

REFERENCES

[1] Silver, R., Germer, T., Attota, R., Barnes, B.M., Bunday, B., Allgair, J., Marx, E. and Jun, J., "Fundamental limits of optical critical dimension metrology: a simulation study," Proc. SPIE 6518, 65180U (2007).

[2] Germer, T.A., Patrick, H. J., Silver, R. M. and Bunday, B. , "Developing an Uncertainty Analysis for Optical Scatterometry," in this volume, (2009).

[3] Boher, P., Petit, J., Leroux, T., Foucher, J., Desieres, Y., Hazart, J. and Chaton, P., "Optical Fourier transform scatterometry for LER and LWR metrology," Proc. SPIE 5752, 192-203 (2005).

[4] Germer, T. A., "Effect of line and trench profile variation on specular and diffuse reflectance from a periodic structure," J. Opt. Soc. Am. A 24(3), 696-701 (2007).

[5] Moharam, M. G., Pommet, D. A., Grann, E. B. and Gaylord, T. K., "Stable Implementation Of The Rigorous Coupled-Wave Analysis For Surface-Relief Gratings - Enhanced Transmittance Matrix Approach," J. Opt. Soc. Am. A 12(5), 1077-1086 (1995).

[6] Moharam, M. G., Grann, E. B., Pommet, D. A. and Gaylord, T. K., "Formulation For Stable And Efficient Implementation Of The Rigorous Coupled-Wave Analysis Of Binary Gratings," J. Opt. Soc. Am. A 12(5), 1068-1076 (1995).

[7] Li, L. F., "Use of Fourier series in the analysis of discontinuous periodic structures," J. Opt. Soc. Am. A 13(9), 1870-1876 (1996).

[8] Lalanne, P. and Morris, G. M., "Highly improved convergence of the coupled-wave method for TM polarization," J. Opt. Soc. Am. A 13(4), 779-784 (1996).

[9] Germer, T.A., "Modeled Integrated Scatter Tool (MIST)" Available from: http://physics.nist.gov/scatmech (2009).

[10] Li, L., "New formulation of the Fourier modal method for crossed surface-relief gratings," J. Opt. Soc. Am. A 14(10), 2758-2767 (1997).

[11] Bohren, C.F. and Huffman, D.R., [Absorption and scattering of light by small particles], Wiley-VCH, 141-148, (2004).

[12] Ronnow, D., Anderson, S. K. and Niklasson, G. A., "Surface roughness effects in ellipsometry: Comparison of truncated sphere and effective medium models," Optical Materials 4(6), 815-821 (1995).

[13] Tomkins, H. G., [A User's Guide to Ellipsometry], Academic Press, 246-252 (1993).

[14] Aspnes, D. E., Theeten, J. B. and Hottier, F., "Investigation of effective-medium models of microscopic surface roughness by spectroscopic ellipsometry," Physical Review B 20(8), 3292-3302 (1979).

[15] Born, M. and Wolf, E., [Principles of Optics: Electromagnetic Theory of Propagation, Interference and Diffraction of Light - 7th Edition], New York: Cambridge University Press, New York, 837-840 (1999).

[16] Yariv, A. and Yeh, P., "Electromagnetic propagation in periodic stratified media. II. Birefringence, phase matching, and x-ray lasers," J. Opt. Soc. Am 67(4), 438-448 (1976).

[17] Southwell, W. H., "Pyramid-array surface-relief structures producing antireflection index matching on optical surfaces," J. Opt. Soc. Am 8(3), 549-553 (1991).

[18] Rytov, S. M., “Electromagnetic properties of a finely stratified medium,” Sov. Phys. JETP 2, 466–475 (1956).

[19] Bischoff, J., Drege, E., and Yedur, S., "Edge roughness measurement in optical metrology", USPTO 7,046,375 B2 , Timbre Technology, Inc. (2006)

[20] Bevinton, P. R. and Robinson, D. K., [Data Reduction and Analysis for the Physical Sciences], McGraw Hill, Boston, 104-107 (2003).